

## RESEARCH ARTICLE

# Biodegradation of poly(ester-urethane) coatings by *Halopseudomonas formosensis*

Jan de Witt<sup>1</sup>  | Rebecka Molitor<sup>2</sup>  | Jochem Gätgens<sup>1</sup>  |  
 Claire Ortmann de Percin Northumberland<sup>3</sup>  | Luzie Kruse<sup>2</sup>  |  
 Tino Polen<sup>1</sup>  | Benedikt Wynands<sup>1</sup>  | Koen van Goethem<sup>4</sup>  |  
 Stephan Thies<sup>2</sup>  | Karl-Erich Jaeger<sup>1,2</sup>  | Nick Wierckx<sup>1</sup> 

<sup>1</sup>Institute of Bio- and Geosciences IBG-1: Biotechnology, Forschungszentrum Jülich, Jülich, Germany

<sup>2</sup>Institute of Molecular Enzyme Technology, Heinrich-Heine-University Düsseldorf, Forschungszentrum Jülich, Jülich, Germany

<sup>3</sup>Ernst Ruska-Centre for Microscopy and Spectroscopy with Electrons: ER-C-3: Structural Biology, Forschungszentrum Jülich, Jülich, Germany

<sup>4</sup>I-COATS N.V., Antwerp, Belgium

## Correspondence

Nick Wierckx, Institute of Bio- and Geosciences IBG-1: Biotechnology, Forschungszentrum Jülich, Jülich, Germany.  
 Email: [n.wierckx@fz-juelich.de](mailto:n.wierckx@fz-juelich.de)

## Funding information

German Federal Ministry of Education and Research, Grant/Award Number: 031B0852B and 031B867B; Bio-based Industries Joint Undertaking (JU), Grant/Award Number: 887711; European Union's Horizon 2020 research and innovation programme

## Abstract

Impranil® DLN-SD is a poly(ester-urethane) (PEU) that is widely used as coating material for textiles to fine-tune and improve their properties. Since coatings increase the complexity of such plastic materials, they can pose a hindrance for sustainable end-of-life solutions of plastics using enzymes or microorganisms. In this study, we isolated *Halopseudomonas formosensis* FZJ due to its ability to grow on Impranil DLN-SD and other PEUs as sole carbon sources. The isolated strain was exceptionally thermotolerant as it could degrade Impranil DLN-SD at up to 50°C. We identified several putative extracellular hydrolases of which the polyester hydrolase *Hfor*\_PE-H showed substrate degradation of Impranil DLN-SD and thus was purified and characterized in detail. *Hfor*\_PE-H showed moderate temperature stability ( $T_m = 53.9^\circ\text{C}$ ) and exhibited activity towards Impranil DLN-SD as well as polyethylene terephthalate. Moreover, we revealed the enzymatic release of monomers from Impranil DLN-SD by *Hfor*\_PE-H using GC-ToF-MS and could decipher the associated metabolic pathways in *H. formosensis* FZJ. Overall, this study provides detailed insights into the microbial and enzymatic degradation of PEU coatings, thereby deepening our understanding of microbial coating degradation in both contained and natural environments. Moreover, the study highlights the relevance of the genus *Halopseudomonas* and especially the novel isolate and its enzymes for future bio-upcycling processes of coated plastic materials.

## INTRODUCTION

Coatings are thin layers of polymers that are applied to the surface of materials to improve their appearance or properties. They are used in a wide range of industries, including fishery, automotive, aerospace, medical and leisure. Many coatings consist of poly(ester-urethane)s (PEUs) that are known for their excellent mechanical properties, including high strength, good fatigue resistance and high abrasion

resistance (Hojabri et al., 2012; Quienne et al., 2020; Ye et al., 2020). Hence, PEUs are used in a variety of coating applications to improve the durability and chemical and biological resistance of these materials. Depending on the chemical composition, coatings can also be used to tune the biodegradability of a material. However, coatings also add to the complexity of a material by increasing the number of polymers it is composed of and, consequently, the number of molecular building blocks. PEUs thus currently pose

This is an open access article under the terms of the [Creative Commons Attribution-NonCommercial](https://creativecommons.org/licenses/by-nc/4.0/) License, which permits use, distribution and reproduction in any medium, provided the original work is properly cited and is not used for commercial purposes.

© 2023 The Authors. *Microbial Biotechnology* published by Applied Microbiology International and John Wiley & Sons Ltd.





a hindrance for the mechanical and chemical recycling of coated plastics. This makes bio-upcycling a promising sustainable end-of-life solution for PEUs, because this technology is potentially suitable for complex polymer and monomer mixtures (Ballerstedt et al., 2021; Sullivan et al., 2022). In this envisioned approach, biological processes depolymerize the entire plastic product including its coating followed by either bio-recycling or bio-upcycling. For this, enzymes and microorganisms able to depolymerize and metabolize PEUs are essential. In addition, many coatings, for instance on fishing nets, are subject to mechanical abrasion which releases them into nature, making the design and understanding of polymer biodegradability of high environmental importance. Thus, PEU coatings are disseminated into the environment and may hinder the recycling of plastics. However, they also have the potential to increase the application range of biodegradable polymers by protecting sensitive materials and tuning surface properties like lubrication, hydrophobicity and abrasion resistance. Hence, it is of great interest to establish sustainable end-of-life solutions of such products by identifying microorganism and enzymes able to depolymerize coatings consisting of PEUs.

One of the best-researched industrial PEU is Impranil® DLN-SD, an anionic aliphatic PEU used for the formulation of textile coatings. Several bacterial and fungal species have been described to degrade Impranil DLN-SD including species of *Pseudomonas* and *Cladosporium* (Álvarez-Barragán et al., 2016; Biffinger et al., 2015; Howard et al., 2001; Howard & Blake, 1998; Russell et al., 2011). Enzymes of such microorganisms were often rashly designated as 'polyurethane-degrading enzyme' or 'polyurethanase' without confirmation that the urethane (carbamate) bond was hydrolysed. Instead, these enzymes only showed polyester hydrolase activity, solubilizing the polymer by cleaving the ester bonds present in the PEU but leaving the urethane bond intact. Hence, these enzymes should be classified as extracellular esterases or lipases. So far, no enzymes with true polyurethane depolymerizing activities are scientifically described (Liu et al., 2021; Wei et al., 2020). Instead, certain urethanases and cutinases are known to cleave only PU oligomers (Akutsu-Shigeno et al., 2006; Branson et al., 2023). Nonetheless, oxidative enzymes exist that are capable of depolymerizing PU, but in an unspecific mode (Magnin et al., 2021). Most enzymes known to depolymerize the ester bonds of Impranil DLN-SD were originally identified as polyethylene terephthalate (PET) hydrolases, including cutinases such as the leaf and branch compost cutinase (LCC), *Thermobifida fusca* cutinase (TfCut2) (Schmidt et al., 2017), lipases (Rowe & Howard, 2002; Schöne et al., 2016)

or general esterases (Magnin et al., 2020). Recently, it was shown that members of the niche-adapted genus *Halopseudomonas* possess extracellular type IIa PET-hydrolases (PE-H) that are able to hydrolyse Impranil DLN-SD (Molitor et al., 2020). Furthermore, the PE-H of *Halopseudomonas aestusnigri* (*Haes-PE-H*) and *Halopseudomonas bauzanensis* were shown to be active towards PET (Avilan et al., 2023; Bollinger, Thies, Katzke, & Jaeger, 2020; Bollinger, Thies, Knieps-Grünhagen, et al., 2020). However, bacterial growth of *Halopseudomonas* spp. with Impranil DLN-SD as sole carbon source has not been investigated and the metabolic pathways of Impranil DLN-SD degradation remain unknown, until now. The lack of established tools for genetic engineering of this genus further complicates the process of investigating the metabolic routes in detail.

In this study, we aimed to identify and characterize novel microorganisms and enzymes for PEU degradation. For this, we performed enrichment cultures that led to the isolation of the Impranil DLN-SD-metabolizing bacterium *Halopseudomonas formosensis* FZJ. The characterization of this strain and its extracellular hydrolases highlights their potential for biodegradation of several PEUs and gives insights into the corresponding metabolic pathways. Moreover, this study reports the first genetic modification within the genus *Halopseudomonas* leading the path for exploring this niche-adapted and biotechnologically relevant genus.

## EXPERIMENTAL PROCEDURES

### Strain isolation and cultivation

*H. formosensis* FZJ was isolated from a mesophilic compost heap in Würselen, Germany (50.8351551, 6.1411361). For the initial enrichment, mineral salts medium (MSM) (Wierckx et al., 2005) was inoculated with 10 g L<sup>-1</sup> of compost material and 1% (v/v) Impranil DLN-SD (Covestro AG, Leverkusen, Germany). Shake flasks were incubated at 30°C and 200 rpm shaking speed. After 3 days, the flasks were re-inoculated into fresh MSM medium supplemented with 1% (v/v) Impranil DLN-SD. After five re-inoculations, different species were isolated on lysogeny broth (LB) agar plates containing 1% (v/v) Impranil DLN-SD. The isolate exhibiting the strongest halo formation was selected for this study and in the following termed *Halopseudomonas formosensis* FZJ. Strains of *Escherichia coli* were cultivated in LB medium with appropriate antibiotics if necessary. For cultivation of *H. formosensis* FZJ, 10 mM of suberic acid was added to LB medium to facilitate growth. All strains used in this study are shown in Table 1.



TABLE 1 Strains used in this study.

Strains	Description	References
<i>Halopseudomonas formosensis</i> FZJ	Wild-type isolate	This study
<i>Escherichia coli</i> strains		
HB101 pRK2013	$F^-$ <i>mcrB mrr hsdS20(rB^- mB^-) recA13 leuB6 ara-14 proA2 lacY1 galK2 xyl-5 mtl-1 rpsL20(Sm<sup>R</sup>) gln V44λ<sup>-</sup></i>	Boyer and Roulland-Dussoix (1969)
PIR2 pEMG-Δ <i>Hfor</i> _PE-H	$F^-$ Δ <i>lac169 rpoS</i> (Am) <i>robA1 creC510 hsdR514 endA reacA1 uidA</i> (Δ <i>Mlui</i> ):: <i>pir</i>	This study
EPI400 pQT8- <i>scel</i>	$F^-$ <i>mcrA</i> Δ( <i>mrr-hsdRMS-mcrBC</i> ) <i>φ80dlacZΔM15 ΔlacX74 recA1 endA1 araD139 Δ(ara, leu)7697 galU galK λ-rpsL nupG tonA ΔpcnBdhf</i>	This study
LOBSTR	$F^-$ <i>ompT gal dcm lon hsdSB(rB^- mB^-) λ(DE3 [lacI lacUV5-T7 gene 1 ind1 sam7 nin5]) Δ(ArnA SlyD)</i>	Andersen et al. (2013)
LOBSTR pET21a_Δ <i>Hfor</i> _PE-H	$F^-$ <i>ompT gal dcm lon hsdSB(rB^- mB^-) λ(DE3 [lacI lacUV5-T7 gene 1 ind1 sam7 nin5]) Δ(ArnA SlyD)</i>	This study
LOBSTR pET22b_Δ <i>Haes</i> _PE-H	$F^-$ <i>ompT gal dcm lon hsdSB(rB^- mB^-) λ(DE3 [lacI lacUV5-T7 gene 1 ind1 sam7 nin5]) Δ(ArnA SlyD)</i>	This study
LOBSTR pET22b_Δ <i>Haes</i> _PE-H Y250S	$F^-$ <i>ompT gal dcm lon hsdSB(rB^- mB^-) λ(DE3 [lacI lacUV5-T7 gene 1 ind1 sam7 nin5]) Δ(ArnA SlyD)</i>	This study
LOBSTR pET21a_Δ <i>sPETase</i>	$F^-$ <i>ompT gal dcm lon hsdSB(rB^- mB^-) λ(DE3 [lacI lacUV5-T7 gene 1 ind1 sam7 nin5]) Δ(ArnA SlyD)</i>	This study

## 16S rDNA sequencing

For preliminary identification of the isolated strain, 16S rDNA sequencing was performed. Genomic DNA was purified using a Monarch Genomic DNA Purification Kit (NEB) from an overnight LB culture of single colonies. The 16S rDNA sequence was amplified by PCR using Q5 High-Fidelity 2× Master Mix (NEB) as DNA polymerase and the primers FD1/2 (5′-3′ AGAGTTTG ATCMTGGCTCAG) and RP1/2 (5′-3′ ACGGYTAC CTTGTTACGACTT) (Weisburg et al., 1991). PCR products were purified with a Monarch PCR and DNA Cleanup Kit (NEB) and sequenced by Eurofins Genomics (Ebersberg, Germany). The resulting sequences were aligned to the nucleotide collection (nr/nt) of the NCBI database using BLASTn and hits with the highest sequence identities were compared (Sayers et al., 2022).

## Whole genome sequencing

Genomic DNA from strains of interest was purified using a Monarch Genomic DNA Purification Kit (NEB) from an overnight LB culture. Afterwards, 1 μg of DNA was used for library preparation using the NEBNext Ultra™ II DNA Library Prep Kit for Illumina (NEB). The library was evaluated by qPCR using the KAPA library quantification kit (Peqlab, Erlangen, Germany). Afterwards, normalization for pooling was done and paired-end sequencing with a read length of 2×150 bases was performed on a MiSeq (Illumina). The reads

of demultiplexed fastq files as the sequencing output (base calls) were trimmed and quality-filtered using the CLC Genomic Workbench software (Qiagen Aarhus A/S, Aarhus, Denmark). Then, the filtered reads were used for de novo assembly using the CLC Genomic Workbench software. Sequencing data are stored in the NCBI Sequence Read Archive under the BioProject number PRJNA987411 under accession number SRR25019772. The annotated genome of *H. formosensis* FZJ can be accessed via the accession number JAVRDO000000000.

## Quantification of NH<sub>4</sub><sup>+</sup> consumption

The turbidity of Impranil DLN-SD in aqueous media prevented to analyse bacterial growth via the optical density (OD<sub>600</sub>). Hence, the consumption of NH<sub>4</sub><sup>+</sup> was chosen as suitable parameter as it correlates with bacterial growth. For quantifying the NH<sub>4</sub><sup>+</sup> consumption, a colorimetric assay was adapted from Willis et al. (1996). The NH<sub>4</sub><sup>+</sup> concentration was reduced to 300 mg L<sup>-1</sup> in the MSM for cultivation. Samples from liquid cultivations were filtered through an AcroPrep™ 96-well filter plate (Pall Corporation, Port Washington, NY, USA) to obtain the analytes for the assay. In a 96-well plate, 10 μL of analytes (0.5–50 mg L<sup>-1</sup> NH<sub>4</sub><sup>+</sup>) was mixed with 200 μL of reagent A (32 g L<sup>-1</sup> Na-salicylate, 40 g L<sup>-1</sup> Na<sub>3</sub>PO<sub>4</sub> × 12 H<sub>2</sub>O and 0.5 g L<sup>-1</sup> sodium nitroprusside (Na<sub>2</sub>[Fe(CN)<sub>5</sub>NO] × 2 H<sub>2</sub>O)). After that, 50 μL of reagent B (0.25% (v/v) NaClO) was added and mixed. Samples were incubated at room temperature for 20 min and subsequently the absorbance was detected at λ = 685 nm



using a Tecan infinite M nano plate reader (Tecan Group, Männedorf, Schweiz).

## Genetic engineering

The mutant  $\Delta Hfor\_PE-H$  derived from *H. formosensis* FZJ was constructed using the I-SceI-based system (Martínez-García & de Lorenzo, 2011) according to the streamlined protocol (Wynands et al., 2018) and further optimized to allow genetic engineering of *H. formosensis* FZJ. The 500–600 bp up- and downstream flanking regions (TS1 and TS2) of the *Hfor\\_PE-H* encoding gene (RED13\_000930) were integrated into the suicide delivery vector pEMG. The integration of the suicide vector into *H. formosensis* FZJ was performed by patch mating for 24 h on LB agar plates. For this, the *E. coli* PIR2 donor strain holding the pEMG- $\Delta Hfor\_PE-H$  plasmid, the helper strain *E. coli* HB101 pRK2013, and the recipient *H. formosensis* FZJ were used. To enable expression of *sce-I*, we constructed pQT8-*sce-I* that was recognized by *H. formosensis* FZJ after electroporation. For this, the strain was cultivated in LB medium supplemented with 10 mM suberic acid at 30°C overnight. Next, the cells were harvested by centrifugation at 16,000 g for 1 min. The cell pellet was resuspended in half of the initial volume with 300 mM sucrose. After two additional washing steps, cells were resuspended in 2% of the initial volume in 300 mM sucrose. Next, 1 µg of pQT8-*sce-I* was added to 50 µL of cells and electroporation was performed using DEVICE X (0.2 cm cuvette, 2.5 kV, 25 µF and 200 Ω). After the electroporation, 950 µL of LB medium supplemented with 10 mM suberic acid was added and cells were regenerated at 30°C for 5 h. Transformed cells were selected on LB agar plates containing 20 mg L<sup>-1</sup> gentamicin. The successful knock-out of *Hfor\\_PE-H* was confirmed by DNA sequencing.

## Microscopic analysis

Light microscopy pictures were taken on an AxioImager M2 equipped with a Zeiss AxioCam MRm camera and an C Plan-Neofluar 100×/1.3 Oil Ph3 objective (Carl Zeiss, Germany). Images were analysed using the AxioVision 4.8 software (Carl Zeiss). For Transmission Electron Microscopy, *H. formosensis* FZJ was cultivated with Impranil in MSM for 72 h and was adsorbed on CF300-Cu grids (Electron microscopy services) and negatively stained with 2% uranyl acetate. Staining procedure by side blotting was carried out as described in Ohi et al. (2004). TEM images were acquired on a Talos L120C G2 transmission

electron microscope (Thermo Fisher Scientific) operated at 120 keV with a 4k×4k Ceta 16M CMOS camera.

## GC-ToF-MS analysis

For sample preparation, cultures were filtered through an AcroPrep™ 96-well filter plate to obtain cell-free filtrates (Pall Corporation, Port Washington, NY, USA). Aliquots of 130 µL were shock-frozen in liquid nitrogen and stored at -20°C. Prior to analysis, samples were lyophilized overnight in a Christ LT-105 freeze drier (Martin Christ Gefriertrocknungsanlagen, Osterode am Harz, Germany). Two-step derivatization of the samples and GC-ToF-MS analysis was performed as described before by Paczia et al. (2012) using a L-PAL3-S15 liquid auto sampler coupled to a LECO GCxGC HRT+ 4D high resolution time-of-flight mass spectrometer (LECO, Mönchengladbach, Germany). To identify known metabolites, a baseline noise-corrected fragmentation pattern together with the corresponding current RI value (Retention time Index) was compared to our in-house accurate *m/z* database JuPoD and the commercial nominal *m/z* database NIST20 (National Institute of Standards and Technology, USA). Unknown peaks were identified by a virtual reconstruction of the derivatized metabolite structure via the measured baseline noise-corrected accurate mass *m/z* fragmentation pattern in comparison to an accurate *m/z* fragmentation register inside the JuPoD main library and were subsequently verified by virtual derivatization and fragmentation of the predicted structure.

## Enzyme production and purification

The expression plasmids including the enzyme-encoding genes were codon-optimized for *E. coli* and ordered from Twist Bioscience, USA and subsequently rehydrated according to the manufacturer protocol. Protein production and purification was carried out according to Bollinger, Thies, Katzke, and Jaeger (2020) and Bollinger, Thies, Knieps-Grünhagen, et al. (2020) with minor changes. For heterologous expression, the *E. coli* strain LOBSTR was used (Andersen et al., 2013). For this, a pre culture was cultivated with 0.5% (w/v) glucose for 24 h at 37°C. From this, the main culture was inoculated with a starting OD<sub>580</sub> of 0.05 and incubated at 30°C for 24 h under agitation of 160 rpm. The cells were then harvested and purified according to Bollinger, Thies, Katzke, and Jaeger (2020) and Bollinger, Thies, Knieps-Grünhagen, et al. (2020).



## Biochemical characterization

Esterase activity was measured using 4-nitrophenyl hexanoate as substrate. The substrate solution was prepared from a stock solution of 20 mM 4-nitrophenyl hexanoate in acetonitrile mixed 1/20 with 100 mM potassium phosphate buffer with 100 mM NaCl (pH 7.2). Ten microliter of the enzyme solution was mixed with 190  $\mu$ L of the substrate solution in a microtiter plate and immediately measured at 30°C/40°C/50°C in Tecan Infinite M1000Pro (Tecan Trading AG, Switzerland) or Molecular Devices SpectraMax iD3 (Molecular Devices, USA) photometers at 410 nm for 10 min with a measurement every 22 s. The volumetric esterase activity was calculated using

the formula 
$$\frac{\Delta OD_{410} [\text{min}^{-1}] * \text{vol. in MTP} [\text{mL}] * \text{dilution factor}}{d [\text{cm}] * \epsilon [\text{mM}^{-1} * \text{cm}^{-1}] * \text{sample volume} [\text{mL}]}$$

\* enzyme concentration  $\left[ \frac{\text{mg}}{\text{mL}} \right] = \frac{U}{\text{mg}}$  (Nolasco-Soria et al., 2018).

## Determination of protein thermal melting point

The melting curves of the proteins were measured using nano differential scanning fluorimetry (nanoDSF) using a Prometheus device (NanoTemper Technologies, Inc.). The NanoTemper capillaries were loaded with purified enzyme at a concentration of about 1 mg mL<sup>-1</sup> in 100 mM potassium phosphate buffer with 100 mM NaCl (pH 7.2). The melting temperature was scanned in a range between 20 and 99°C at a rate of 1°C per minute.

## Enzymatic hydrolysis of PET and quantification of reaction products

The hydrolysis of PET films and powder, was determined as described by Bollinger, Thies, Katzke, and Jaeger (2020) and Bollinger, Thies, Knieps-Grünhagen, et al. (2020) with minor modifications. The reaction mixture in a total volume of 200  $\mu$ L was composed of 1 mg mL<sup>-1</sup> purified enzyme in 100 mM potassium phosphate buffer with 100 mM NaCl (pH 7.2) with 20% (v/v) dimethyl sulfoxide (DMSO) and a circular piece of PET film (6 mm diameter, Goodfellow Cambridge, Ltd.) or 5 mg of powdered amorphous PET film. The reaction mixtures were incubated in centrifugal filters with a cut-off (MWCO) of 10,000 Da (VWR International GmbH) for a total of 96 h at 30°C. Every 24 h 50  $\mu$ L of the solution was harvested by centrifugation at 18,900 g for 30 s and frozen at -20°C until use. The reaction filtrates were analysed with an UPLC system (Acquity UPLC, Waters GmbH) equipped with an Acquity UPLC BEH C18 column (1.7  $\mu$ m particle size) using the published method by (Bollinger, Thies, Katzke, & Jaeger, 2020);

Bollinger, Thies, Knieps-Grünhagen, et al., 2020). For terephthalic acid (TA) and BHET, commercially available standards were used to calculate amounts from calibration curves. For MHET, standards were used generated by the Winde lab of the University of Leiden (The Netherlands) and kindly made available to us.

## Enzymatic hydrolysis of Impranil DLN-SD

Degradation of Impranil DLN-SD was determined by measuring the decrease in optical density at 580 nm (Islam et al., 2019). Ten microliter of enzyme solution were mixed with 190  $\mu$ L of substrate solution consisting of 100 mM potassium phosphate buffer with 100 mM NaCl (pH 7.2) and 1% (v/v) Impranil DLN-SD. The final enzyme concentration used in the assays was 50 nM. The loss of turbidity was then measured in a Tecan Infinite M1000Pro (Tecan Trading AG, Switzerland) or Molecular Devices SpectraMax iD3 (Molecular Devices, USA) photometer at a wavelength of 580 nm for 10 min at 30, 40 and 50°C with measurement intervals every 22 s. The absolute value of the calculated slope was used as a measure of activity.

## RESULTS AND DISCUSSION

### Isolation of poly(ester-urethane)-degrading *Halopseudomonas formosensis* FZJ

PEU-degrading bacteria were isolated from soil samples obtained from a composting facility. For this, enrichment cultures were grown in mineral salts medium (MSM) supplemented with 1% (v/v) Impranil DLN-SD as sole carbon source at 30°C. After repetitive inoculation for two weeks, the enriched organisms were isolated on lysogeny broth (LB) agar plates containing 1% (v/v) Impranil DLN-SD. Two isolated strains showed remarkable halo formation indicating the secretion of PEU-degrading enzymes (Figure 1A). 16S rDNA sequencing of the isolates classified them as a *Bacillus* sp. and *Halopseudomonas formosensis*. The 16S rDNA of the latter shares a sequence identity of 99.92% to that of *H. formosensis* CC-CY503<sup>T</sup> (Lin et al., 2013). This genus was recently re-classified from *Pseudomonas* into the novel *Halopseudomonas* lineage (Bollinger, Thies, Katzke, & Jaeger, 2020; Bollinger, Thies, Knieps-Grünhagen, et al., 2020; Peix et al., 2018; Rudra & Gupta, 2021). Many Halopseudomonads harbour a PE-H, among them *H. aestusnigri* (Haes-PE-H) degrading not only Impranil DLN-SD but also PET (Bollinger, Thies, Katzke, & Jaeger, 2020; Bollinger, Thies, Knieps-Grünhagen, et al., 2020; Molitor et al., 2020). Since halo formation and growth on Impranil DLN-SD of the isolated *H. formosensis* strain, designated as



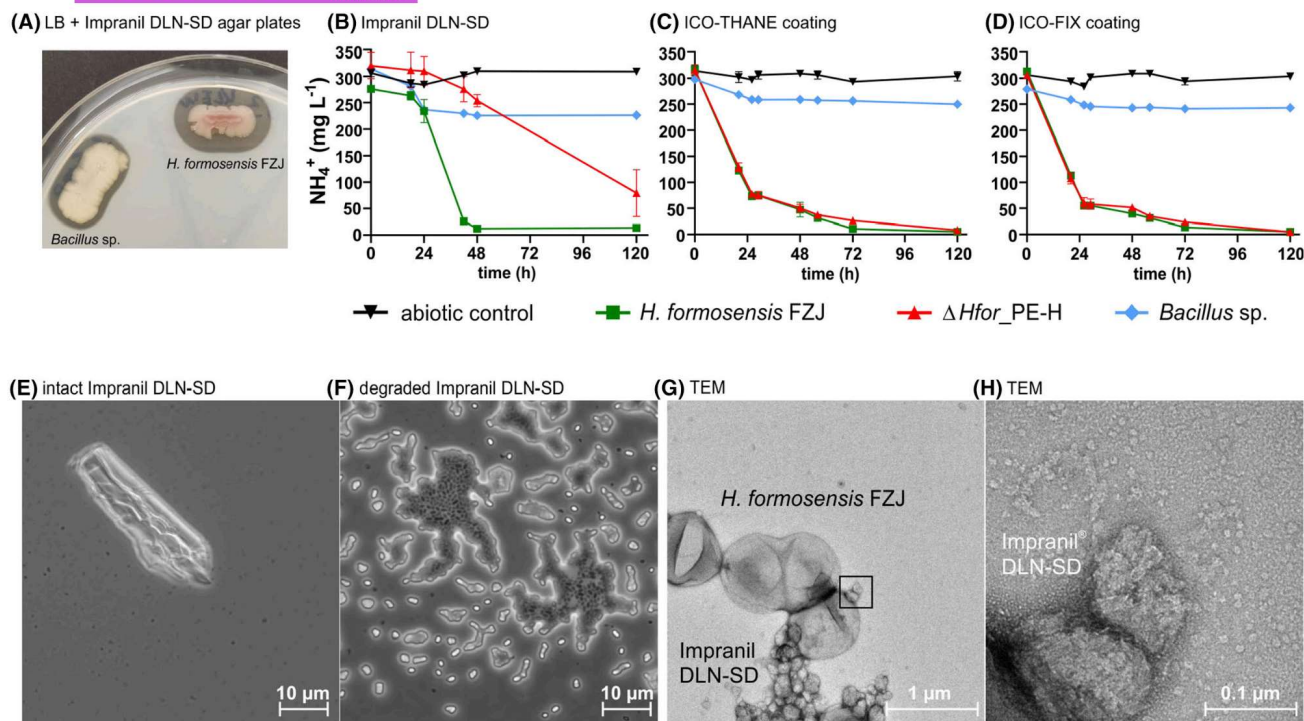


**FIGURE 1** Growth of *Halopseudomonas formosensis* FZJ with different PEUs. Halo formation of the two isolated strains on LB agar plates containing 1% (v/v) Impranil DLN-SD (A). The wild-type *H. formosensis* FZJ, its knock-out mutant of *Hfor\\_PE-H* ( $\Delta Hfor\_PE-H$ ) and the *Bacillus* sp. isolate were cultivated at 30°C in mineral salts medium (MSM) supplemented with 1% (v/v) Impranil DLN-SD (B), 1% (w/v) ICO-THANE coating (C) or 1% (w/v) ICO-FIX coating (D) as sole carbon source. An abiotic control lacking a bacterial isolate was included. Impranil DLN-SD was added as dispersion and the ICO-THANE and ICO-FIX coatings were added in powdered form. Growth was analysed by measuring the consumption of ammonium ( $\text{NH}_4^+$ ). The mean values and standard deviation (SD) of three replicates are displayed. Light microscopy of MSM cultures supplemented with 1% (v/v) Impranil DLN-SD without (E) and with (F) *H. formosensis* FZJ was performed after 72h. The same *H. formosensis* FZJ culture was analysed by transmission electron microscopy (TEM) with negative staining (G and H). The presence of *H. formosensis* FZJ and Impranil DLN-SD is indicated as well as the image section that was zoomed into for figure H ((G), black square).

*H. formosensis* FZJ, was stronger compared to that of the *Bacillus* sp. isolate (Figure 1A,B), whole-genome sequencing (WGS) of *H. formosensis* FZJ was performed to screen for putative hydrolases. Genome analysis led to the identification of a PE-H homologue in *H. formosensis* FZJ (*Hfor\\_PE-H*) that shared a protein sequence identity of 99.7% with the putative PE-H from *H. formosensis* CC-CY503<sup>T</sup> and of 80.3% with the characterized PET-degrading *Haes\\_PE-H*. Including *Hfor\\_PE-H*, a total number of 24 hydrolases were identified of which 14 were predicted to contain a signal peptide (Table S1). Such secreted hydrolases may be well suited to extracellularly break down the polymer into monomers and oligomers that are imported and metabolized by *H. formosensis* FZJ.

The presence of a secreted PE-H and the ability to grow on agar plates containing Impranil DLN-SD indicated that *H. formosensis* FZJ is able to metabolize the PEU. Growth experiments with Impranil DLN-SD as sole carbon source confirmed the ability of the isolate to metabolize the coating (Figure 1B). Since the turbidity of Impranil DLN-SD interfered with the optical density ( $\text{OD}_{600}$ ) that is usually used as parameter for monitoring growth, the consumption of  $\text{NH}_4^+$  was

utilized to quantify bacterial growth using a colorimetric assay (Willis et al., 1996). Moreover, the increase in colony forming units during the cultivation with Impranil DLN-SD as sole carbon source confirmed growth of *H. formosensis* FZJ with the polymeric substrate (Figure S1). *H. formosensis* FZJ was unable to grow on Impranil DLN-SD when no  $\text{NH}_4^+$  was present in the medium, indicating that Impranil was not utilized as nitrogen source. Hence, no urethanase is likely present in this strain resulting in intact carbamate bonds within the polymer.

To investigate whether *Hfor\\_PE-H* was responsible for Impranil DLN-SD degradation, we aimed to delete the encoding gene to test its effect on growth on the polymer. However, members of the genus *Halopseudomonas* were thus far not genetically accessible. Hence, we adapted the streamlined I-Scel-based system that is well established for engineering the genus *Pseudomonas* (Martínez-García & de Lorenzo, 2011; Wynands et al., 2018). Since *oriRK2* of traditional *sce-I* expression plasmids, such as pSW-2, was not recognized by *H. formosensis* FZJ, we enabled expression of *sce-I* by constructing pQT8-*sce-I* that harboured the pRO1600 origin of replication. Indeed,



pQT8-*sce-I* was able to replicate in *H. formosensis* FZJ and thus enabled deletion of the target gene resulting in the  $\Delta Hfor\_PE-H$  mutant. This mutant showed impaired growth on Impranil DLN-SD, thus confirming its activity towards the polymer (Figure 1B). Since growth of the  $\Delta Hfor\_PE-H$  mutant was not entirely abolished, at least one of the remaining 13 putative secreted hydrolases must also possess an activity towards Impranil. Moreover, a synergistic effect of *Hfor\\_PE-H* with further secreted hydrolases is conceivable as the polymer consists of various ester and urethane bonds that might be favoured by different hydrolases. Hence, cleavage of oligomers might be favoured by other hydrolases than *Hfor\\_PE-H* analogous to the synergy of PET- and MHETases during PET depolymerization (Yoshida et al., 2016).

Light microscopy confirmed the breakdown of refractive Impranil DLN-SD by *H. formosensis* FZJ into smaller particles (Figure 1E–H). Moreover, cells of *H. formosensis* FZJ seemed to be attached to the polymer suggesting that membrane-bound hydrolases may contribute to polymer degradation (Figure 1F–H). Using Transmission Electron Microscopy (TEM), the size of *H. formosensis* FZJ was detected to be approximately  $1\ \mu\text{m} \times 0.5\ \mu\text{m}$  (Figure 1G).

Besides Impranil DLN-SD, two solid coatings provided by I-COATS N.V (Antwerp, Belgium) were also metabolized by *H. formosensis* FZJ (Figure 1C,D), showing the versatile applicability of this strain for coating degradation. These two commercial bio-based PEU coatings find application in the textile and fishing gear industry and belong to the ICO-THANE and ICO-FIX family coatings, respectively. To simulate realistic biodegradation conditions, they were applied to a surface, removed, and micronized before inoculation. Interestingly, the  $\Delta Hfor\_PE-H$  mutant showed no growth defects compared to the wild type when cultivated with these coatings. This could be explained by the presence of triacylglycerides in these materials. Other secreted hydrolases might degrade these compounds and thus circumvent the need of *Hfor\\_PE-H* when degrading the ICO-THANE and ICO-FIX coating. After 72h of cultivation, both ICO-THANE and ICO-FIX coatings were completely depolymerized into the soluble fraction as no solid particles were observed.

The majority of Halopseudomonads grow at temperatures between 4 and 37°C (Bollinger, Thies, Katzke, & Jaeger, 2020; Bollinger, Thies, Knieps-Grünhagen, et al., 2020), whereas *H. formosensis* CC-CY503<sup>T</sup> was reported to grow in a range of 20–50°C (Lin et al., 2013). To compare the Impranil DLN-SD-degrading activities within this genus at different temperatures, various strains were cultivated on LB and MSM agar plates containing 1% (v/v) Impranil DLN-SD. Halo formation on LB indicates the ability to secrete PEU-degrading enzymes, while growth and/or halo formation on MSM

indicates the use of Impranil DLN-SD as sole carbon source. On LB agar plates all tested strains were able to degrade Impranil at 30°C (Figure 2A). However, only *H. formosensis* FZJ degraded the polymer at 40 and 50°C. On MSM agar plates, *H. formosensis* FZJ showed the strongest halo formation at 30°C among the tested strains (Figure 2B). When the temperature was increased to 40°C, *H. formosensis* FZJ was the only strain still able to grow on Impranil. However, no growth or halo formation was detected when *H. formosensis* FZJ was cultivated on MSM agar plates containing Impranil at 50°C. Overall, these results reveal *H. formosensis* FZJ as thermotolerant strain able to secrete enzymes and degrade Impranil at higher temperatures compared to other Halopseudomonads. As *H. formosensis* FZJ features a relatively high GC content of 62.8% compared to the other tested strains of this genus (58.5%–60.5%) this might be a potential factor contributing to its increased thermotolerance. Moreover, the increased thermotolerance of *H. formosensis* FZJ likely originates

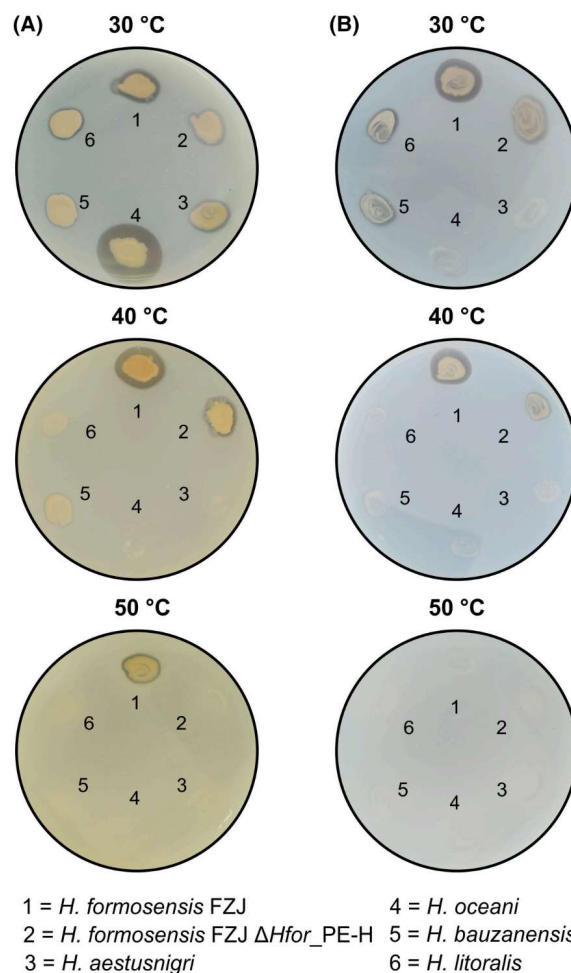


**FIGURE 2** Temperature-dependent growth of *Halopseudomonas* spp. on Impranil DLN-SD agar plates. Strains were cultivated on lysogeny broth (LB) agar plates (A) or mineral salts medium (MSM) agar plates (B) containing 1% (v/v) Impranil DLN-SD at the indicated temperature for 4 days.



from the compost environment from which it was isolated, which usually encounters higher temperatures than the environment of other *Halopseudomonads* such as the ocean or soil (Bollinger, Thies, Katzke, & Jaeger, 2020; Bollinger, Thies, Knieps-Grünhagen, et al., 2020). Thermostable enzymes and microorganisms are favoured for depolymerization due to the increased polymer chain mobility at elevated temperatures increasing the bioavailability and thus biodegradability of polymers (Sullivan et al., 2022; Tokiwa et al., 2009; Tsuji & Miyauchi, 2001). Although *H. formosensis* FZJ is not a thermophilic organism, its thermotolerance compared to other *Halopseudomonads* and Impranil-degrading species can contribute to increased biodegradability of PEU coatings.

### Biochemical characterization of *Hfor*\_PE-H

Given that *H. formosensis* FZJ is able to grow on Impranil DLN-SD at higher temperatures than other *Halopseudomonads*, we aimed to characterize *Hfor*\_PE-H in comparison to other related enzymes in this regard. Therefore, *Hfor*\_PE-H as well as the closely related *Haes*\_PE-H (Bollinger, Thies, Katzke, & Jaeger, 2020; Bollinger, Thies, Knieps-Grünhagen, et al., 2020) and the well-known PETase from *Ideonella sakainensis* (*IsPETase*) (Yoshida et al., 2016) were heterologously expressed and purified for *in vitro* studies. The temperature stabilities were assessed using a Prometheus NanoTemper with a gradient from 20 to 99°C. In this analysis *Hfor*\_PE-H ( $T_m = 53.9^\circ\text{C}$ ) did not show exceptionally

high temperature stability compared to *Haes*\_PE-H ( $55.6^\circ\text{C}$ ) (Figure 3A), indicating that the superior performance at higher temperature results from the thermotolerance of *H. formosensis* FZJ on the cellular level as compared to *H. aestusnigri*.

As indicated by the  $\Delta Hfor\_PE-H$  mutant, *Hfor*\_PE-H showed polyester-degrading activities that were further analysed *in vitro*. For this, the decrease of Impranil DLN-SD turbidity was measured over time, which corresponds to the hydrolytic activity and depolymerization of the substrate. *Hfor*\_PE-H showed similar activities at 30 and 40°C whereas the activity decreased approximately two-fold at 50°C (Figure 3B). Compared to *Haes*\_PE-H, *Hfor*\_PE-H showed a slightly higher activity at all tested temperatures. Notably, Impranil DLN-SD incubated with *IsPETase* underwent a visible change in appearance that did not result in a decrease of turbidity measured at 580 nm. It might be speculated that this enzyme catalysed transesterification reactions under the applied assay condition. Interestingly, with the model substrate 4-nitrophenyl hexanoate (4-NPH), *Hfor*\_PE-H showed a remarkable increase in activity at 50°C (Figure 3C). This might be explained by temperature-dependent substrate properties that could affect the activity of *Hfor*\_PE-H.

Since *H. formosensis* FZJ showed growth on different polyesters, we also tested whether *Hfor*\_PE-H can degrade PET. For this, *Hfor*\_PE-H was incubated for 168 h at 30°C with either an amorphous PET film or an amorphous PET foil that was ground to a powder. For the ground PET powder, *Hfor*\_PE-H released minor amounts of PET monomers MHET and terephthalate (TA) (Figure 4A), while almost no activity was detected with the less accessible PET foil (Figure 4B). Overall,

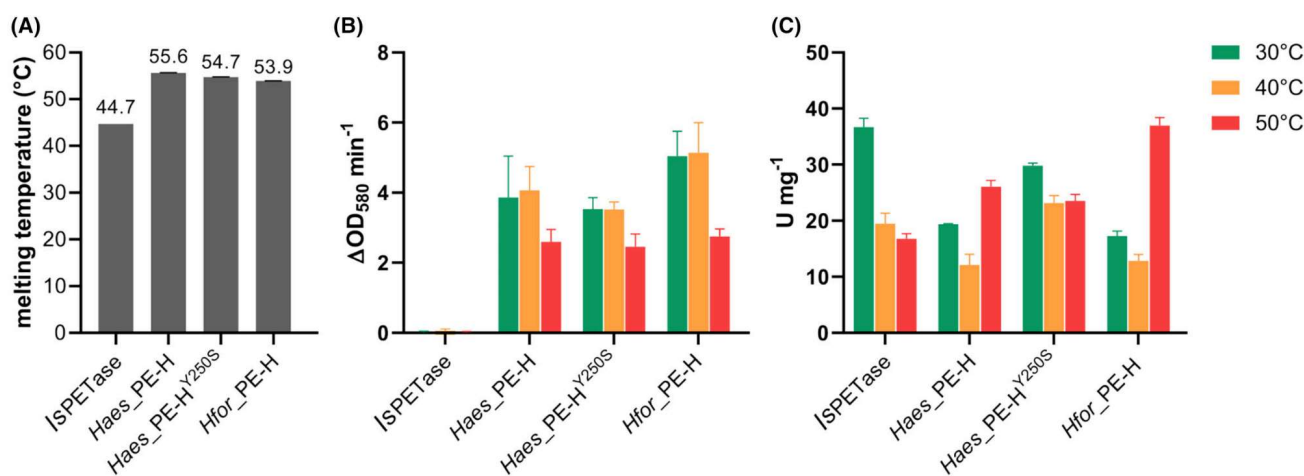


**FIGURE 3** Temperature-dependent activity of *Hfor*\_PE-H. (A) Melting temperatures of the *Hfor*\_PE-H in comparison with *IsPETase* and *Haes*\_PE-H. All *Halopseudomonas*-derived PE-Hs showed increased structural melting temperatures indicating thermostability. (B) Activity of *Hfor*\_PE-H and other hydrolases towards Impranil DLN-SD at different temperatures over 10 min with enzyme concentrations of 50 nM. The activity is shown as the absolute decrease of turbidity determined as absorption at a wavelength of 580 nm per minute. As Impranil DLN-SD is a suspension, a reaction time of 10 min was sufficient to observe polymer degradation. Exemplary plots of turbidity decrease over time are displayed in Figure S2. (C) Activity of *Hfor*\_PE-H and other hydrolases towards 4-nitrophenyl hexanoate. The activity was measured over the course of 10 min. Error bars indicate the standard deviation (SD) of two replicates.



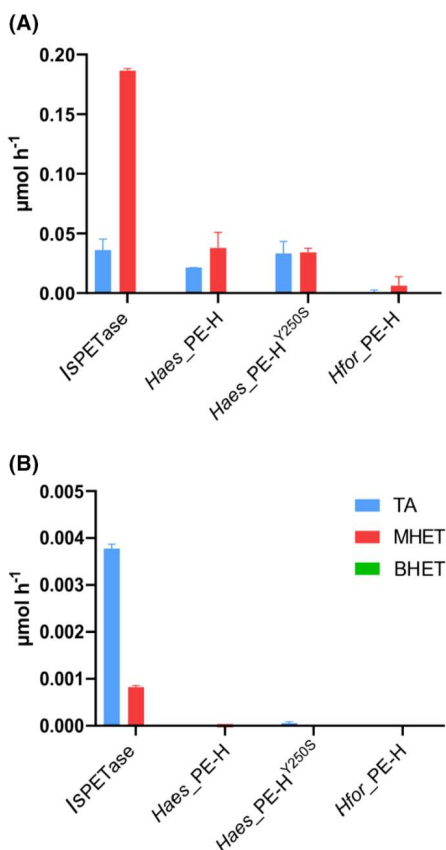


**FIGURE 4** Activity of *Hfor*\_PE-H towards PET substrates. Release of the monomers terephthalate (TA), mono-(2-hydroxyethyl)terephthalate (MHET) and bis-(2-hydroxyethyl)terephthalate (BHET) after incubation with (A) powdered amorphous PET foil or (B) an amorphous PET film for 168 h at 30°C.

*Hfor*\_PE-H showed a higher activity towards Impranil DLN-SD but lower activities towards 4-NPH and PET compared to *IsPETase* and *Haes*\_PE-H. This is in line with the fact that *H. formosensis* FZJ was isolated by selection for growth on Impranil DLN-SD.

## Microbial metabolism of poly(ester-urethanes)

The extracellular cleavage of Impranil DLN-SD by *Hfor*\_PE-H and the ability to grow on the polymer indicated the release of low molecular weight compounds that were metabolized by *H. formosensis* FZJ. Although the exact composition of Impranil DLN-SD is unknown, Howard et al. (2012) proposed that it is made of poly hexane/neopentyl adipate polyester and hexamethylene diisocyanate. To investigate whether *H. formosensis* FZJ metabolizes these putative monomers of Impranil DLN-SD, the strain was cultivated in MSM supplemented with various aliphatic dicarboxylates, diamines and diols as sole carbon source. None of the investigated diols or diamines with chain-lengths from C<sub>4</sub> to C<sub>8</sub> were metabolized (Figure 5A). In contrast to

this, dicarboxylates with a chain length of six or higher were metabolized by *H. formosensis* FZJ with a preference for the long-chain C<sub>8</sub>-, C<sub>9</sub>- and C<sub>10</sub>-dicarboxylates (Figure 5B). These results suggested that *H. formosensis* FZJ mainly metabolizes long-chain dicarboxylates that might originate from Impranil DLN-SD hydrolysed by *Hfor*\_PE-H. A protein homology search of the genome of *H. formosensis* FZJ identified genes encoding homologues to the dicarboxylic acid (Dca) metabolic proteins from *Acinetobacter baylyi* ADP1 involved in the metabolism of aliphatic dicarboxylates (Ackermann et al., 2021; Parke et al., 2001). The identified Dca homologues were encoded in a nine-gene and a two-gene operon in *H. formosensis* FZJ (Figure 5C). Due to the additional presence of a CoA carboxylase and a hydroxymethylglutaryl-CoA lyase within the identified nine-gene operon, it is likely that the encoded pathway enables the metabolism of acyclic terpenes but it might show side activities for long-chain dicarboxylate substrates (Jurado et al., 2015). Additionally, a putative transporter, encoded by RED13\_001611, was identified that could import such dicarboxylates. The transporter showed a protein sequence identity of 25.8% towards the *cis,cis*-muconate transport protein (Muck) from *A. baylyi* ADP1 that imports a variety of dicarboxylic acids including muconate and terephthalate (Pardo et al., 2020; Parke et al., 2001). Due to the broad substrate spectrum of Muck and the fact that no homologue of the dicarboxylate transport system DcaKP was discovered in the genome of *H. formosensis* FZJ, the identified transporter likely contributed to the import of C<sub>6</sub>- to C<sub>10</sub>-dicarboxylates. Future studies will be needed to investigate the role of the identified Dca homologues and the putative dicarboxylate transporter to confirm their role in Impranil DLN-SD metabolism.

To further unravel the metabolic pathways for growth on Impranil DLN-SD by *H. formosensis* FZJ, gas chromatography time-of-flight mass spectrometry (GC-ToF-MS) was performed on supernatants of both *in vivo* cultures and *in vitro* *Hfor*\_PE-H assays. *In vitro* depolymerization of Impranil DLN-SD by *Hfor*\_PE-H resulted in the release of four monomers, namely neopentyl glycol, 1,6-hexanediol, adipic acid and an unknown compound designated as M\_162 (Figures 6A, 7). These results match the structure of Impranil DLN-SD proposed by Howard et al., with the polyester region of the polymer consisting of poly hexane diol/neopentyl adipate polyester. The absence of (di-) amines after enzymatic hydrolysis confirms the inability of *Hfor*\_PE-H to hydrolyse the urethane bonds within the polymer. Growth of *H. formosensis* FZJ with Impranil DLN-SD resulted in the accumulation of neopentyl glycol that is in agreement with the inability of the strain to metabolize this monomer (Figures 5A, 6B). Although adipic acid was metabolized by *H. formosensis* FZJ, it was still present in the culture supernatant, indicating that it was released



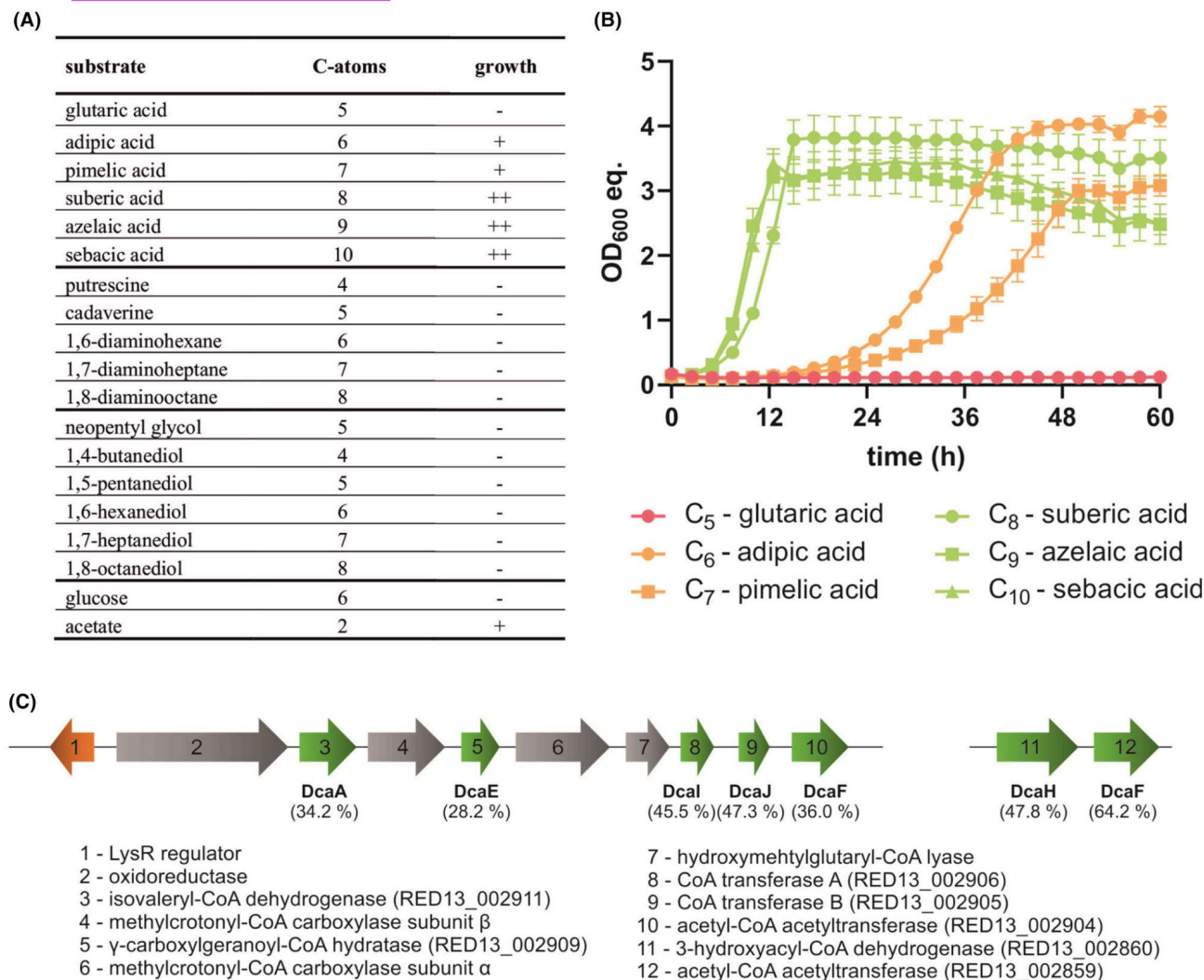


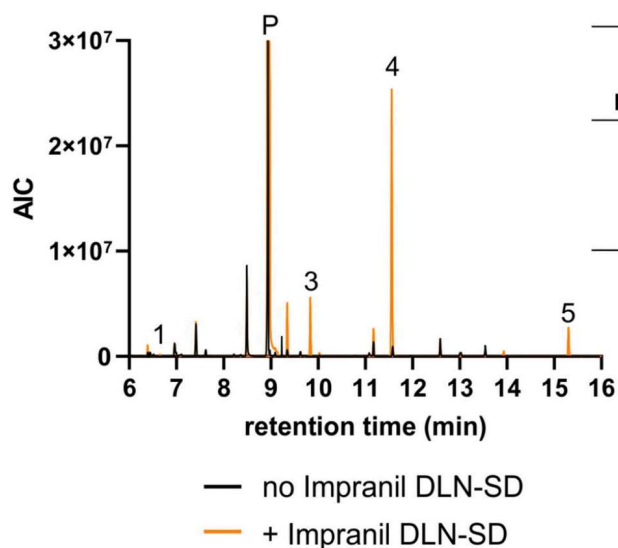
**FIGURE 5** Substrate range of *Halopseudomonas formosensis* FZJ. The strain was cultivated in a Growth Profiler 960 in 96-well microtiter plates in mineral salts medium (MSM) supplemented with the indicated substrate at concentrations that were the C-mol equivalent of 30 mM adipic acid. (A) Overview of the investigated substrates. Growth time needed to reach the stationary phase within 18 h (++) , 48 h (+) or no growth (-). (B) Growth of *H. formosensis* FZJ in MSM with aliphatic dicarboxylic acids as sole carbon source. The mean values and standard deviations (SD) of three replicates are shown. (C) Putative gene clusters encoding enzymes for the metabolism of dicarboxylic acids in *H. formosensis* FZJ. Homologous genes of the *dca* cluster from *Acinetobacter baylyi* ADP1 are shown in green with their corresponding protein sequence identity. Orange indicates a putative regulator of this cluster. Genes are numbered according to the indicated gene products and locus tags of the respective genes are displayed in brackets.

by *Hfor*\_PE-H faster than it could be metabolized (Figure 7). Moreover, 1,6-hexanediol was detected and, indeed, this compound could not be metabolized by *H. formosensis* FZJ as sole carbon source (Figures 5A, 6A). 4-Hydroxybutyrate was detected in the culture supernatant, but not in the enzymatically treated sample. This hydroxylated acid is thus unlikely to be a constituent of Impranil DLN-SD, rather, it is a possible intermediate of aliphatic diol metabolism (Li et al., 2020), indicating that *H. formosensis* FZJ can partially oxidize the diols (Figure 7). The fact that the putative precursor 1,4-butanediol was not detected in any sample suggests that the 4-hydroxybutyrate originates from partial  $\beta$ -oxidation of 1,6-hexanediol. An unknown compound (M\_162) was also detected in the culture supernatant of *H. formosensis* FZJ.

Mass spectral analysis of M\_162 revealed the chemical formula  $C_7H_{14}O_4$  and the detected fragmentation pattern indicates that this compound could be a dimer of neopentyl glycol and glycolic acid namely 3-hydroxy-2,2-dimethylpropyl 2-hydroxyacetate (Figure S3). The presence of such a dimer in the culture supernatant supports our theory that hydrolases other than *Hfor*\_PE-H might degrade the released oligomers. However, it can only be speculated whether 3-hydroxy-2,2-dimethylpropyl 2-hydroxyacetate is cleaved extracellularly or imported into the cell for subsequent metabolism (Figure 7). The absence of glycolic acid in the culture supernatant might indicate that the oligomer is directly imported without prior cleavage into neopentyl glycol and glycolic acid. The presence of many genes encoding intracellular

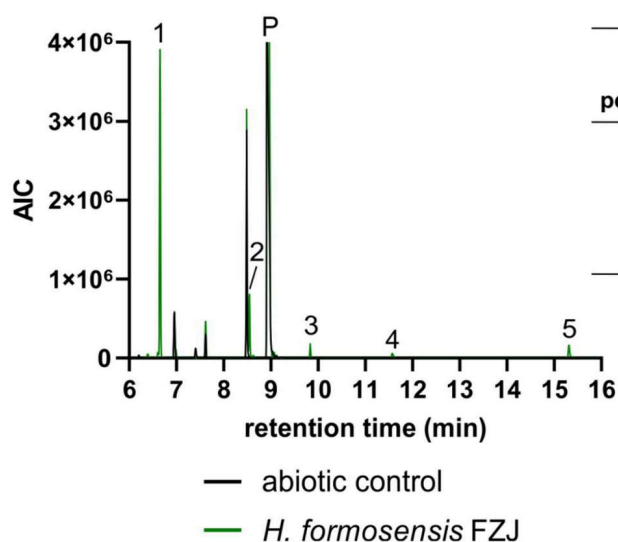


## (A) Enzymatic degradation



peak	compound	R. T. (min)	no Impranil® DLN-SD TIC area (%)	+ Impranil® DLN-SD TIC area (%)
1	neopentyl glycol	6.65	n. d.	0.1
3	1,6-hexanediol	9.84	n. d.	1.4
4	adipic acid	11.56	n. d.	6.6
5	M_162	15.30	n. d.	0.8

## (B) Microbial degradation



peak	compound	R. T. (min)	abiotic control TIC area (%)	<i>H. formosensis</i> FZJ TIC area (%)
1	neopentyl glycol	6.65	n. d.	2.6
2	4-hydroxybutyrate	8.85	n. d.	0.8
3	1,6-hexanediol	9.84	n. d.	0.2
4	adipic acid	11.56	n. d.	0.2
5	M_162	15.30	n. d.	0.2

**FIGURE 6** GC-ToF-MS analysis of Impranil DLN-SD degradation. (A) Chromatogram of in vitro depolymerized Impranil DLN-SD (orange) and its negative control not containing the polymer (black) showing the analytical ion current (AIC) over the time. Peaks of released monomers are labelled and summarized in the corresponding table with their annotation, retention time (R. T.) and relative area of the total ion current (TIC). Mass spectral analysis indicated that M\_162 might be 3-hydroxy-2,2-dimethylpropyl 2-hydroxyacetate (Figure S3). Compounds that were not detected in a sample are labelled with 'n. d.' and P indicates the dominant phosphate peak. Samples were incubated with *Hfor*\_PE-H in 100 mM potassium phosphate buffer (pH 7.2) containing 100 mM NaCl with or without 1% (v/v) Impranil DLN-SD at 30°C for 1 h. (B) Chromatogram of in vivo depolymerized Impranil DLN-SD by *H. formosensis* FZJ (green) and its abiotic control (black). Samples were incubated in mineral salts medium supplemented with 1% (v/v) Impranil DLN-SD at 30°C for 72 h. A full list of all detected compounds is shown in Table S2.

hydrolases in *H. formosensis* FZJ supports the theory of oligomer import and intracellular cleavage of them (Table S1).

Overall, our results unravelled the metabolic pathway for Impranil DLN-SD in *H. formosensis* FZJ. First, *Hfor*\_PE-H and putatively other hydrolases are secreted for initial polymer degradation. Enzymatic degradation of the ester segments

results in the release of neopentyl glycol, adipate and 1,6-hexanediol of which only adipate was metabolized by the strain via the identified  $\beta$ -oxidation pathway. Moreover, short oligomers such as 3-hydroxy-2,2-dimethylpropyl 2-hydroxyacetate are likely imported into the cell and might be substrates for intracellular hydrolases (Figure 7). Future genetic engineering of *H. formosensis* FZJ could expand



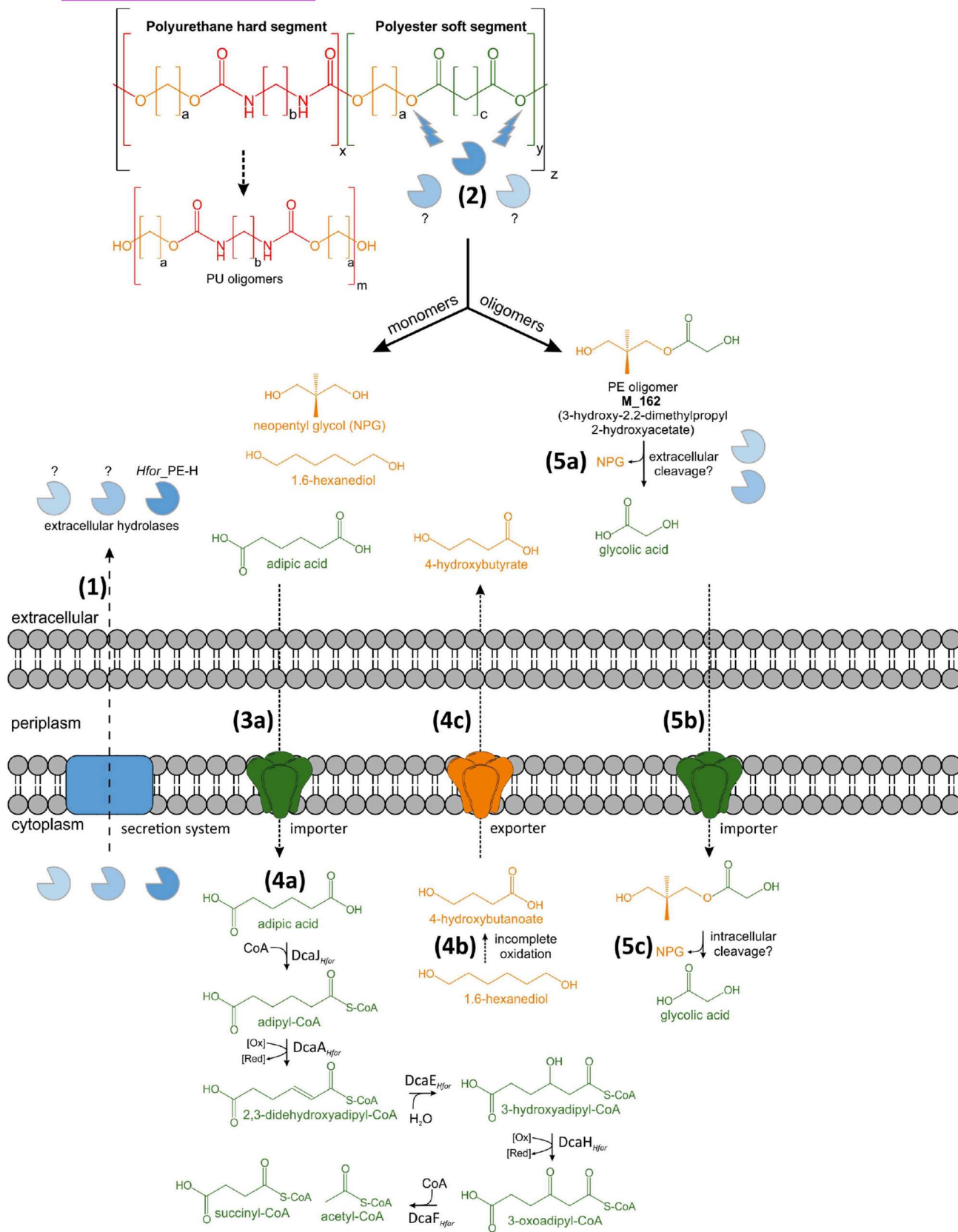


**FIGURE 7** Proposed metabolic pathways for Impranil DLN-SD degradation by *H. formosensis* FZJ. (1) Secretion of extracellular hydrolases including *Hfor*-PE-H via the Sec protein translocation system. (2) Enzymatic hydrolysis of ester bonds within the polyester segment by *Hfor*-PE-H and other extracellular hydrolases. Enzymatic hydrolysis releases large oligomers of polyurethane (PU) as well as monomers and oligomers that were detected via GC-ToF-MS. (3a) Import of monomers and subsequent metabolism of adipic acid via  $\beta$ -oxidation (4a). (4b) Incomplete oxidation of 1,6-hexanediol and export of the dead-end product 4-hydroxybutyrate (4c). 3-hydroxy-2,2-dimethylpropyl 2-hydroxyacetate (M<sub>162</sub>) was identified as polyester (PE) oligomer released upon in vivo degradation of *H. formosensis* FZJ. It is conceivable that this compound is cleaved extracellularly (5a) or imported into the cell (5b) for intracellular cleavage by hydrolases (5c).



its metabolism by heterologous expression of urethanases and implementation of metabolic routes for monomers such as 1,6-hexanediol or neopentyl glycol (Branson et al., 2023). Considering these modifications, *H. formosensis* FZJ has the great potential to function as platform strain for bio-upcycling of PEU coatings with increasing genetic accessibility of Halopseudomonads.

## CONCLUSION AND OUTLOOK

PEU coatings, such as Impranil DLN-SD, are indispensable for tuning and improving the properties of the plastic materials they are applied on. However, they pose a hindrance for chemical or mechanical recycling. Biodegradation of such coatings is a powerful strategy to overcome these hurdles by using enzymes or microorganisms capable of depolymerizing the protective coating layer. In this study, *H. formosensis* FZJ was isolated for its ability to grow on Impranil DLN-SD and was also able to metabolize ICO-THANE and ICO-FIX PEU coatings as sole carbon source. In contrast to other Halopseudomonads, *H. formosensis* FZJ showed an outstanding temperature tolerance and was able to depolymerize Impranil DLN-SD at up to 50°C making it a promising candidate for industrial processes. The identified *Hfor*\_PE-H showed higher activity towards Impranil DLN-SD compared to its homologues within the phylogenetic lineage. Deletion of the corresponding gene led to impaired growth on Impranil DLN-SD and constitutes the first report of a genetic modification of a *Halopseudomonas* bacterium. Overall, the detailed characterization of Impranil DLN-SD metabolism indicated rapid degradation, but only partial metabolization of the PEU coating by *H. formosensis* FZJ. The profound knowledge on both microorganism and enzymes in this study contributes to the understanding of the interaction of microbes with synthetic polymers. Hence, this study leads the path for future bio-recycling strategies aiming for recycling entire plastic materials including their coatings.

## AUTHOR CONTRIBUTIONS

**Jan de Witt:** Investigation (lead); methodology (lead); visualization (lead); writing – original draft (equal); writing – review and editing (equal). **Rebecka Molitor:** Investigation (equal); writing – original draft (equal). **Jochem Gätgens:** Investigation (supporting); resources (supporting). **Claire Ortmann de Percin Northumberland:** Investigation (supporting); resources (supporting). **Luzie Kruse:** Resources (supporting). **Tino Polen:** Investigation (supporting); resources (supporting). **Benedikt Wynands:** Writing – review and editing (supporting). **Koen van Goethem:** Resources (supporting). **Stephan Thies:** Conceptualization (equal); supervision (equal); writing – review and editing

(supporting). **Karl-Erich Jaeger:** Supervision (supporting); writing – review and editing (equal). **Nick Wierckx:** Conceptualization (lead); funding acquisition (lead); supervision (lead); writing – review and editing (equal).

## ACKNOWLEDGEMENTS

This project has received funding from the Bio-based Industries Joint Undertaking (JU) under the European Union's Horizon 2020 research and innovation programme under grant agreement No 887711. The JU receives support from the European Union's Horizon 2020 research and innovation programme and the Bio-based Industries Consortium. This work was in part supported by the German Federal Ministry of Education and Research (BMBF) via the projects PlastiSea (031B867B) and NO-STRESS (031B0852B). We thank Covestro AG for providing Impranil DLN-SD and Kompostanlage Würselen for providing soil samples. We thank Jo-Anne Maurits-Verschoor from the University of Leiden, The Netherlands, for providing the MHET standard. We thank the electron microscopy training, imaging and access time granted by the life science EM facility of the Ernst-Ruska Centre at Forschungszentrum Jülich for TEM analysis. Open Access funding enabled and organized by Projekt DEAL.

## CONFLICT OF INTEREST STATEMENT


I-COATS is the producer and purveyor of ICO-THANE and ICO-FIX. The authors declare that there are no further conflicts of interest.

## DATA AVAILABILITY STATEMENT

Data will be made available upon request. Sequencing data are stored in the NCBI Sequence Read Archive under the BioProject number PRJNA987411 under accession number SRR25019772. The annotated genome of *H. formosensis* FZJ is stored under accession number JAVRDO000000000.

## ORCID

Jan de Witt  <https://orcid.org/0000-0003-2799-1097>

Rebecka Molitor  <https://orcid.org/0000-0002-9925-7038>

Jochem Gätgens  <https://orcid.org/0000-0002-9232-180X>

Claire Ortmann de Percin Northumberland  <https://orcid.org/0000-0002-2989-1463>

Luzie Kruse  <https://orcid.org/0000-0003-4224-9755>

Tino Polen  <https://orcid.org/0000-0002-0065-3007>

Benedikt Wynands  <https://orcid.org/0000-0001-8599-3205>

Stephan Thies  <https://orcid.org/0000-0003-4240-9149>

Karl-Erich Jaeger  <https://orcid.org/0000-0002-6036-0708>

Nick Wierckx  <https://orcid.org/0000-0002-1590-1210>

Stephan Thies  <https://orcid.org/0000-0003-4240-9149>

Karl-Erich Jaeger  <https://orcid.org/0000-0002-6036-0708>

Nick Wierckx  <https://orcid.org/0000-0002-1590-1210>

Stephan Thies  <https://orcid.org/0000-0003-4240-9149>

Karl-Erich Jaeger  <https://orcid.org/0000-0002-6036-0708>

Nick Wierckx  <https://orcid.org/0000-0002-1590-1210>

Stephan Thies  <https://orcid.org/0000-0003-4240-9149>



## REFERENCES

- Ackermann, Y.S., Li, W.J., Op de Hipt, L., Niehoff, P.J., Casey, W., Polen, T. et al. (2021) Engineering adipic acid metabolism in *Pseudomonas putida*. *Metabolic Engineering*, 67, 29–40.
- Akutsu-Shigeno, Y., Adachi, Y., Yamada, C., Toyoshima, K., Nomura, N., Uchiyama, H. et al. (2006) Isolation of a bacterium that degrades urethane compounds and characterization of its urethane hydrolase. *Applied Microbiology and Biotechnology*, 70, 422–429.
- Álvarez-Barragán, J., Domínguez-Malfavón, L., Vargas-Suárez, M., González-Hernández, R., Aguilar-Osorio, G. & Loza-Tavera, H. (2016) Biodegradative activities of selected environmental fungi on a polyester polyurethane varnish and polyether polyurethane foams. *Applied and Environmental Microbiology*, 82, 5225–5235.
- Andersen, K.R., Leksa, N.C. & Schwartz, T.U. (2013) Optimized *E. coli* expression strain LOBSTR eliminates common contaminants from his-tag purification. *Proteins*, 81, 1857–1861.
- Avilan, L., Lichtenstein, B.R., König, G., Zahn, M., Allen, M.D., Oliveira, L. et al. (2023) Concentration-dependent inhibition of mesophilic PETases on poly(ethylene terephthalate) can be eliminated by enzyme engineering. *ChemSusChem*, 16, e202202277.
- Ballerstedt, H., Tiso, T., Wierckx, N., Wei, R., Averous, L., Bornscheuer, U. et al. (2021) MIXed plastics biodegradation and UPcycling using microbial communities: EU horizon 2020 project MIX-UP started January 2020. *Environmental Sciences Europe*, 33, 99.
- Biffinger, J.C., Barlow, D.E., Cockrell, A.L., Cusick, K.D., Hervey, W.J., Fitzgerald, L.A. et al. (2015) The applicability of Impraniil® DLN for gauging the biodegradation of polyurethanes. *Polymer Degradation and Stability*, 120, 178–185.
- Bollinger, A., Thies, S., Katzke, N. & Jaeger, K.-E. (2020) The biotechnological potential of marine bacteria in the novel lineage of *pseudomonas pertucinogena*. *Microbial Biotechnology*, 13, 19–31.
- Bollinger, A., Thies, S., Knieps-Grünhagen, E., Gertzen, C., Kobus, S., Höppner, A. et al. (2020) A novel polyester hydrolase from the marine bacterium *Pseudomonas aestusnigri* – Structural and functional insights. *Frontiers in Microbiology*, 11, 1–16.
- Boyer, H.W. & Roulland-Dussoix, D. (1969) A complementation analysis of the restriction and modification of DNA in *Escherichia coli*. *Journal of Molecular Biology*, 41, 459–472.
- Branson, Y., Sörtl, S., Buchmann, C., Wei, R., Schaffert, L., Badenhorst, C.P.S. et al. (2023) Urethanases for the enzymatic hydrolysis of low molecular weight carbamates and the recycling of polyurethanes. *Angewandte Chemie International Edition*, 62, e202216220.
- Hojabri, L., Jose, J., Leao, A.L., Bouzidi, L. & Narine, S.S. (2012) Synthesis and physical properties of lipid-based poly(ester-urethane)s, I: effect of varying polyester segment length. *Polymer*, 53, 3762–3771.
- Howard, G.T. & Blake, R.C. (1998) Growth of *Pseudomonas fluorescens* on a polyester-polyurethane and the purification and characterization of a polyurethanase-protase enzyme. *International Biodeterioration & Biodegradation*, 42, 213–220.
- Islam, S., Apitius, L., Jakob, F., & Schwaneberg, U. (2019) Targeting microplastic particles in the void of diluted suspensions. *Environment International*, 123, 428–435. <https://doi.org/10.1016/j.envint.2018.12.029>
- Howard, G.T., Crother, B. & Vicknair, J. (2001) Cloning, nucleotide sequencing and characterization of a polyurethanase gene (*pueB*) from *Pseudomonas chlororaphis*. *International Biodeterioration & Biodegradation*, 47, 141–149.
- Howard, G.T., Norton, W.N. & Burks, T. (2012) Growth of *Acinetobacter gerveri* P7 on polyurethane and the purification and characterization of a polyurethanase enzyme. *Biodegradation*, 23, 561–573.
- Jurado, A.R., Huang, C.S., Zhang, X., Zhou, Z.H. & Tong, L. (2015) Structure and substrate selectivity of the 750-kDa  $\alpha 6\beta 6$  holoenzyme of geranyl-CoA carboxylase. *Nature Communications*, 6, 8986.
- Li, W.-J., Narancic, T., Kenny, S.T., Niehoff, P.-J., O'Connor, K., Blank, L.M. et al. (2020) *Unraveling 1,4-Butanediol metabolism in Pseudomonas putida KT2440*. *Microbiol. Front.*, p. 11.
- Lin, S.-Y., Hameed, A., Liu, Y.-C., Hsu, Y.-H., Lai, W.-A. & Young, C.-C. (2013) *Pseudomonas formosensis* sp. nov., a gamma-proteobacteria isolated from food-waste compost in Taiwan. *International Journal of Systematic and Evolutionary Microbiology*, 63, 3168–3174.
- Liu, J., He, J., Xue, R., Xu, B., Qian, X., Xin, F. et al. (2021) Biodegradation and up-cycling of polyurethanes: Progress, challenges, and prospects. *Biotechnology Advances*, 48, 107730.
- Magnin, A., Entzmann, L., Pollet, E. & Avérous, L. (2021) Breakthrough in polyurethane bio-recycling: an efficient laccase-mediated system for the degradation of different types of polyurethanes. *Waste Management*, 132, 23–30.
- Magnin, A., Pollet, E., Phalip, V. & Avérous, L. (2020) Evaluation of biological degradation of polyurethanes. *Biotechnology Advances*, 39, 107457.
- Martínez-García, E. & de Lorenzo, V. (2011) Engineering multiple genomic deletions in gram-negative bacteria: analysis of the multi-resistant antibiotic profile of *Pseudomonas putida* KT2440. *Environmental Microbiology*, 13, 2702–2716.
- Molitor, R., Bollinger, A., Kubicki, S., Loeschcke, A., Jaeger, K.-E. & Thies, S. (2020) Agar plate-based screening methods for the identification of polyester hydrolysis by *Pseudomonas* species. *Microbial Biotechnology*, 13, 274–284.
- Nolasco-Soria, H., Moyano-López, F., Vega-Villasante, F., del Monte-Martínez, A., Espinosa-Chaurand, D., Gisbert, E. et al. (2018) Lipase and phospholipase activity methods for marine organisms. In: Sandoval, G. (Ed.) *Lipases and phospholipases: methods and protocols*. New York, NY: Springer New York, pp. 139–167.
- Ohi, M., Li, Y., Cheng, Y. & Walz, T. (2004) Negative staining and image classification — powerful tools in modern electron microscopy. *Biological Procedures Online*, 6, 23–34.
- Paczia, N., Nilgen, A., Lehmann, T., Gätgens, J., Wiechert, W. & Noack, S. (2012) Extensive exometabolome analysis reveals extended overflow metabolism in various microorganisms. *Microbial Cell Factories*, 11, 122.
- Pardo, I., Jha, R.K., Bermel, R.E., Bratti, F., Gaddis, M., McIntyre, E. et al. (2020) Gene amplification, laboratory evolution, and biosensor screening reveal MucK as a terephthalic acid transporter in *Acinetobacter baylyi* ADP1. *Metabolic Engineering*, 62, 260–274.
- Parke, D., Garcia, M.A. & Ornston, L.N. (2001) Cloning and genetic characterization of *dca* genes required for  $\beta$ -oxidation of straight-chain dicarboxylic acids in *Acinetobacter* sp. strain ADP1. *Applied and Environmental Microbiology*, 67, 4817–4827.
- Peix, A., Ramírez-Bahena, M.H. & Velázquez, E. (2018) The current status on the taxonomy of *Pseudomonas* revisited: an update. *Infection, Genetics and Evolution*, 57, 106–116.
- Quienne, B., Kasmí, N., Dieden, R., Caillol, S. & Habibi, Y. (2020) Isocyanate-free fully biobased star polyester-urethanes: synthesis and thermal properties. *Biomacromolecules*, 21, 1943–1951.
- Rowe, L. & Howard, G.T. (2002) Growth of *Bacillus subtilis* on polyurethane and the purification and characterization of a polyurethanase-lipase enzyme. *International Biodeterioration & Biodegradation*, 50, 33–40.
- Rudra, B. & Gupta, R.S. (2021) Phylogenomic and comparative genomic analyses of species of the family *Pseudomonadaceae*:



- proposals for the genera *Halopseudomonas* gen. Nov. and *Atopomonas* gen. nov., merger of the genus *Oblitomonas* with the genus *Thiopseudomonas*, and transfer of some misclassified species of the genus *pseudomonas* into other genera. *International Journal of Systematic and Evolutionary Microbiology*, 71. <https://doi.org/10.1099/ijsem.0.005011>
- Russell, J.R., Huang, J., Anand, P., Kucera, K., Sandoval, A.G., Dantzer, K.W. et al. (2011) Biodegradation of polyester polyurethane by endophytic fungi. *Applied and Environmental Microbiology*, 77, 6076–6084.
- Sayers, E.W., Bolton, E.E., Brister, J.R., Canese, K., Chan, J., Comeau, D.C. et al. (2022) Database resources of the national center for biotechnology information. *Nucleic Acids Research*, 50, D20–d26.
- Schmidt, J., Wei, R., Oeser, T., Dedavid e Silva, L.A., Breite, D., Schulze, A. et al. (2017) Degradation of polyester polyurethane by bacterial polyester hydrolases. *Polymers*, 9, 65.
- Schöne, A.-C., Kratz, K., Schulz, B. & Lendlein, A. (2016) Polymer architecture versus chemical structure as adjusting tools for the enzymatic degradation of oligo( $\epsilon$ -caprolactone) based films at the air-water interface. *Polymer Degradation and Stability*, 131, 114–121.
- Sullivan, K.P., Werner, A.Z., Ramirez, K.J., Ellis, L.D., Bussard, J.R., Black, B.A. et al. (2022) Mixed plastics waste valorization through tandem chemical oxidation and biological funneling. *Science*, 378, 207–211.
- Tokiwa, Y., Calabria, B.P., Ugwu, C.U. & Aiba, S. (2009) Biodegradability of plastics. *International Journal of Molecular Sciences*, 10, 3722–3742.
- Tsuji, H. & Miyauchi, S. (2001) Poly(L-lactide): VI effects of crystallinity on enzymatic hydrolysis of poly(L-lactide) without free amorphous region. *Polymer Degradation and Stability*, 71, 415–424.
- Wei, R., Tiso, T., Bertling, J., O'Connor, K., Blank, L.M. & Bornscheuer, U.T. (2020) Possibilities and limitations of biotechnological plastic degradation and recycling. *Nature Catalysis*, 3, 867–871.
- Weisburg, W.G., Barns, S.M., Pelletier, D.A. & Lane, D.J. (1991) 16S ribosomal DNA amplification for phylogenetic study. *Journal of Bacteriology*, 173, 697–703.
- Wierckx, N.J.P., Ballerstedt, H., de Bont Jan, A.M. & Wery, J. (2005) Engineering of solvent-tolerant *Pseudomonas putida* S12 for bioproduction of phenol from glucose. *Applied and Environmental Microbiology*, 71, 8221–8227.
- Willis, R.B., Montgomery, M.E. & Allen, P.R. (1996) Improved method for manual, colorimetric determination of Total Kjeldahl nitrogen using salicylate. *Journal of Agricultural and Food Chemistry*, 44, 1804–1807.
- Wynands, B., Lenzen, C., Otto, M., Koch, F., Blank, L.M. & Wierckx, N. (2018) Metabolic engineering of *Pseudomonas taiwanensis* VLB120 with minimal genomic modifications for high-yield phenol production. *Metabolic Engineering*, 47, 121–133.
- Ye, S., Xiang, X., Wang, S., Han, D., Xiao, M. & Meng, Y. (2020) Nonisocyanate CO<sub>2</sub>-based poly(ester-co-urethane)s with tunable performances: A potential alternative to improve the biodegradability of PBAT. *ACS Sustainable Chemistry & Engineering*, 8, 1923–1932.
- Yoshida, S., Hiraga, K., Takehana, T., Taniguchi, I., Yamaji, H., Maeda, Y. et al. (2016) A bacterium that degrades and assimilates poly(ethylene terephthalate). *Science*, 351, 1196–1199.

## SUPPORTING INFORMATION

Additional supporting information can be found online in the Supporting Information section at the end of this article.

**How to cite this article:** de Witt, J., Molitor, R., Gätgens, J., Ortmann de Percin Northumberland, C., Kruse, L., Polen, T. et al. (2024) Biodegradation of poly(ester-urethane) coatings by *Halopseudomonas formosensis*. *Microbial Biotechnology*, 17, e14362. Available from: <https://doi.org/10.1111/1751-7915.14362>